

The Sparse Recovery Autoencoder

Shanshan Wu^{1*}, Alexandros G. Dimakis¹, Sujay Sanghavi¹,
Felix X. Yu², Daniel Holtmann-Rice², Dmitry Storcheus²,
Afshin Rostamizadeh², Sanjiv Kumar²,

¹ University of Texas at Austin
{shanshan@, dimakis@austin., sanghavi@mail.}utexas.edu
² Google Research, New York
{felixyu, dhr, dstorcheus, rostami, sanjivk}@google.com

March 23, 2022

Abstract

Linear encoding of sparse vectors is widely popular, but is most commonly data-independent – missing any possible extra (but a-priori unknown) structure beyond sparsity. In this paper we present a new method to learn linear encoders that adapt to data, while still performing well with the widely used ℓ_1 decoder. The convex ℓ_1 decoder prevents gradient propagation as needed in standard autoencoder training. Our method is based on the insight that unfolding the convex decoder into T projected gradient steps can address this issue. Our method can be seen as a data-driven way to learn a compressed sensing matrix. Our experiments show that there is indeed additional structure beyond sparsity in several real datasets. Our autoencoder is able to discover it and exploit it to create excellent reconstructions with fewer measurements compared to the previous state of the art methods.

1 Introduction

Assume we have some unknown data vector $x \in \mathbb{R}^d$. We can observe only a few ($m < d$) linear equations of its entries and we would like to design these projections by creating a measurement matrix $A \in \mathbb{R}^{m \times d}$ such that the projections $y = Ax$ allow exact (or near-exact) recovery of the original vector $x \in \mathbb{R}^d$.

If $d > m$, this is an ill-posed problem in general: we are observing m linear equations with d unknowns, so any vector x' on the subspace $Ax' = y$ satisfies our observed measurements. In this high-dimensional regime, the only hope is to make a structural assumption on x , so that unique reconstruction is possible. A natural approach is to assume that the data vector is sparse. The problem of designing measurement matrices and reconstruction algorithms that recover sparse vectors from linear observations is called Compressed Sensing (CS), Sparse approximation or Sparse recovery theory (see e.g. [Don06, CRT06]).

*This work was done in part while the author was interning at Google Research, New York.

A natural way to recover is to search for the sparsest solution that satisfies the linear measurements:

$$\arg \min_{x' \in \mathbb{R}^d} \|x'\|_0 \quad \text{s.t. } Ax' = y. \quad (1)$$

Unfortunately this problem is NP-hard and for that reason the ℓ_0 norm is relaxed into an ℓ_1 -norm minimization¹

$$D(A, y) := \arg \min_{x' \in \mathbb{R}^d} \|x'\|_1 \quad \text{s.t. } Ax' = y. \quad (2)$$

Remarkably, if the measurement matrix A satisfies some properties (e.g. Restricted Isometry Property (RIP) [Can08] or the nullspace condition (NSP) [Rau10]) it is possible to prove that ℓ_1 minimization produces the same output as the intractable ℓ_0 minimization.

In this paper we are interested in vectors that are not only sparse but have *additional structure* in their support. This extra structure may not be known or a-priori specified. We propose a data-driven algorithm that *learns a good linear measurement matrix A from data samples*. Our linear measurements are subsequently decoded with ℓ_1 minimization to estimate the unknown vector x .

Many real-world sparse datasets have additional structures beyond simple sparsity. For example, in a demographic dataset with (one-hot encoded) categorical features, a person’s income level may be related to their education. Similarly, in a text dataset with bag-of-words representation, it is much more likely for two related words (e.g., football and game) to appear in the same document than two unrelated words (e.g., football and biology). A third example is that in a genome dataset, certain groups of gene features may be correlated. In this paper, the goal is to *learn* a measurement matrix A to leverage such additional structure in a data-driven way.

Our method is an autoencoder for sparse data, with a linear encoder (the measurement matrix) and a complex non-linear decoder. The latent code is the measurement $y \in \mathbb{R}^m$ which forms the bottleneck of the autoencoder that makes the representation interesting. A popular data-driven dimensionality reduction method is Principal Components Analysis (PCA) (see e.g., [Hot33, BGKL15, WBSD16, LWZ17] and the references therein). PCA is also an autoencoder where both the encoder and decoder are linear and learned from samples. Given a data matrix $X \in \mathbb{R}^{n \times d}$ (where each row corresponds to a sample x_i), the optimal linear encoder represents each data point $x \in \mathbb{R}^d$ by its projection onto the top right-singular components of X . As is well-known, PCA provides the lowest mean-squared error when used with a linear recovery decoder. However, when the data is sparse, non-linear recovery algorithms like (2) can yield significantly better performance both in terms of mean squared error as well as other metrics. This is true, as we show, even when the encoder remains linear.

In this paper, we focus on learning a linear encoder for sparse data. Compared to non-linear embedding method such as kernel PCA [MSS⁺99], a linear method enjoys two broad advantages: 1) easy to compute, since it only needs a matrix-vector multiplication; 2) easy to interpret, as every column of the encoding matrix can be viewed as a feature embedding. Interestingly, Arora et al. [AKNV18] recently observe that the popular word embeddings such as GloVe and word2vec [MSC⁺13, PSM14] form a good measurement matrix that gives better sparse recovery performance for text data than random matrices using ℓ_1 -minimization decoder.

¹Other examples of the sparse recovery algorithms are greedy algorithms [TG07], and iterative algorithms such as CoSaMP [NT09], IHT [BD09], and AMP [DMM09].

Given a sparse dataset that has additional (but unknown) structure, our goal is to learn a good measurement matrix A , when the recovery algorithm is ℓ_1 minimization. More formally, given n sparse samples $x_1, x_2, \dots, x_n \in \mathbb{R}^d$, our problem of finding the best A can be formulated as

$$\min_{A \in \mathbb{R}^{m \times d}} f(A), \quad \text{where } f(A) := \sum_{i=1}^n \|x_i - D(A, Ax_i)\|_2^2. \quad (3)$$

Here $D(\cdot, \cdot)$ is the ℓ_1 decoder defined in (2). Unfortunately, there is no easy way to compute the gradient of $f(A)$ with respect to A , due to the optimization problem defining $D(\cdot, \cdot)$. Our main insight, which will be elaborated on in Section 3.1, is that **replacing the ℓ_1 -minimization with a T -step projected subgradient update of it**, results in gradients being computable. In particular, consider the approximate function $\tilde{f}(A) : \mathbb{R}^{m \times d} \mapsto \mathbb{R}$ defined as

$$\tilde{f}(A) := \sum_{i=1}^n \|x_i - \hat{x}_i\|_2^2, \quad \text{where } \hat{x}_i = T\text{-step projected subgradient of } D(A, Ax_i), \text{ for } i \in [n]. \quad (4)$$

As we will show, now it is *possible* to compute the gradients of $\tilde{f}(A)$ with respect to A ; in fact the overall task of doing so becomes structurally similar to an *autoencoder*.

Our contributions can be summarized as follows:

- We design a novel autoencoder, called ℓ_1 -AE, to learn an efficient and compressed representation for structured sparse vectors. Our autoencoder is easy to train and has only two tuning parameters: the encoding dimension m and the network depth T . The architecture of ℓ_1 -AE is inspired by the projected subgradient method of solving ℓ_1 -minimization. While the exact projected subgradient method requires computing the pseudoinverse, we circumvent this by observing that it is possible to replace the expensive pseudoinverse operation by a simple transpose operation without changing the result (see Lemma 1).
- The most surprising result in this paper is we can learn a linear encoder using an unfolded T -step projected subgradient decoder and the learned measurement matrix *still* performs well for the original ℓ_1 -minimization decoder. As shown in Figure 2, our method outperforms the eight baselines in terms of the reconstruction error on the test data. Specifically, compared to random Gaussian matrices, we can compress the original vector to a lower dimension (by a factor of 2-3x) while still being able to *exactly* recover the original vectors from the measurements. This validates the superior ability of our autoencoder in learning and exploiting structural information from data.
- Although our autoencoder is specifically designed for ℓ_1 -minimization decoder, the learned measurement matrix also performs well (and can perform even better) with the model-based decoder [BCDH10] (Figure 3). This further demonstrates the benefit of learning an adaptive measurement matrix from data. As a baseline algorithm, we slightly modify the original model-based CoSaMP algorithm by adding a positivity constraint without changing the theoretical guarantee (Appendix C), which could be of independent interest.

Notation. We use the uppercase letters to denote matrices and the lowercase letters to denote vectors and scalars. Let A^\dagger denote the Moore-Penrose inverse of matrix A , and A^T denote the transpose. The ℓ_p -norm ($p > 0$) of a vector $x \in \mathbb{R}^d$ is defined as $\|x\|_p = (\sum_{i=1}^d x_i^p)^{1/p}$, where x_i is the i -th coordinate. We use I to denote an identity matrix.

2 Related work

We briefly review the relevant work, and highlight the differences compared to our paper.

Model-based compressed sensing (CS). Model-based CS [BCDH10, HIS14] extends the conventional compressed sensing theory by considering more realistic structured models beyond simple sparsity. Model-based CS requires to know the inter-dependencies between the nonzeros a priori, which is not always possible in practice. Our approach, by contrast, does not require any prior knowledge about the structure in the sparse data.

Learning-based measurement design. Most theoretical results in CS are based on random measurement matrices. There are a few approaches proposed to learn a measurement matrix from training data. One approach is to learn a near-isometric embedding that preserves pairwise distance [HSYB15, BSC13]. This approach usually requires computing the pairwise difference vectors, and hence is computationally expensive if both the number of training samples and the dimension are large (which is the setting that we are interested in). Another approach restricts the form of the measurement matrix, e.g., matrices formed by a subset of rows of a given basis matrix. The learning problem becomes selecting the best subset of rows [BLS⁺16, LC16, GML⁺18]. In Figure 2, we compare our method with the learning-based method proposed in [BLS⁺16], and show that our method needs fewer measurements to recover the original vector.

Adaptive CS. In adaptive CS [SN11, ACCD13, MN14], the new measurement is designed based on the previous measurements in order to maximize the the gain of new information. This is in contrast to our setting, where we are given a set of training samples. And our goal is to learn a good measurement matrix to leverage additional structure in the given samples.

Dictionary learning. Dictionary learning [AEB06, MBPS09] is the problem of learning an overcomplete set of basis vectors from data so that every data point (presumably dense) can be represented as a sparse linear combination of the basis vectors. By contrast, this paper focuses on learning a good measurement matrix for structured sparse data.

Sparse coding. The goal of sparse coding [OF96, DE03] is to find the sparse representation of a dense vector, given a fixed family of basis vectors (aka a dictionary). Training a deep neural network to compute the sparse codes becomes popular recently [GL10, SBS15, XWG⁺16, WLH16, MMP⁺17, MB17, HXIW17, ZG17]. Compared to the traditional convex optimization approaches, a trained neural network can produce a good estimate within a fixed computational budget. This is in contrast to our paper, where we focus on learning a good encoding matrix A rather than speeding up the decoding.

Autoencoders. An autoencoder is a popular neural network architecture for unsupervised learning. It has applications in dimensionality reduction [HS06], pre-training [EBC⁺10], image compression and recovery [MDB17, MPB15], denoising [VLL⁺10], and generative modeling [KW14]. In this paper we design a novel autoencoder ℓ_1 -AE for capturing additional structure for data that are sparse in the standard basis (e.g., categorical data and text data).

Unrolling. The idea of unfolding an iterative algorithm (e.g., gradient descent of an optimization problem) into a neural network structure is a natural way of combining both methods [GL10, HRW14, SBS15, XWG⁺16, WLH16, MMP⁺17, MB17, HXIW17, ZG17]. The main difference between the previous works and this paper is that, the previous works seek a good neural network to replace the original optimization-based algorithm (e.g., to perform the inference task), while in this paper we use the unrolling idea to learn a good measurement matrix. The learned measurement matrix will later be used in the original optimization problem

to achieve superior recovery performance.

3 Our algorithm

Recall that our goal is to learn a measurement matrix A completely from the given samples. This is done via training a novel autoencoder neural network, called ℓ_1 -AE . In this section, we will describe the key idea behind the design of ℓ_1 -AE . While it is possible to extend our framework to vectors that are sparse in non-standard (but known) basis, in this paper we focus on the simple setting, where vectors are sparse in the standard basis and are also nonnegative. This is a natural setting for many real-world datasets, e.g., categorical data and text data.

3.1 Intuition

Our design is strongly motivated by the projected subgradient method used to solve an ℓ_1 -norm minimization problem. Consider the following ℓ_1 -norm minimization problem:

$$\min_{x' \in \mathbb{R}^d} \|x'\|_1 \quad \text{s.t. } Ax' = y, \tag{5}$$

where $A \in \mathbb{R}^{m \times d}$ and $y \in \mathbb{R}^m$. We assume that $m < d$ and that A has rank m . One approach² to solving (5) is the projected subgradient method. The update is given by

$$x^{(t+1)} = \Pi(x^{(t)} - \alpha_t g^{(t)}), \quad \text{where } g^{(t)} = \text{sign}(x^{(t)}) \tag{6}$$

where Π denotes the (Euclidean) projection onto the convex set $\{x' : Ax' = y\}$, and $g^{(t)}$ is the subgradient³ of the objective function $\|\cdot\|_1$ at $x^{(t)}$, and α_t is the step size at the t -th iteration. Since A has full row rank, Π has a closed-form solution given by

$$\Pi(z) = \arg \min_h \|h - z\|_2^2 \quad \text{s.t. } Ah = y \tag{7}$$

$$= z + \arg \min_{h'} \|h'\|_2^2 \quad \text{s.t. } Ah' = y - Az \tag{8}$$

$$= z + A^\dagger(y - Az), \tag{9}$$

where $A^\dagger = A^T(AA^T)^{-1}$ is the Moore-Penrose inverse of matrix A . Substituting (9) into (6), and using the fact that $Ax^{(t)} = y$, we get the following update equation

$$x^{(t+1)} = x^{(t)} - \alpha_t(I - A^\dagger A)\text{sign}(x^{(t)}). \tag{10}$$

We use $x^{(1)} = A^\dagger y$ (which satisfies the constraint $Ax' = y$) as the starting point.

As mentioned in the Introduction, our main idea is to replace the solution of an ℓ_1 -minimization decoder given in (5) by a T -step projected subgradient update given in (10). One technical difficulty in simulating (10) using neural networks is backpropagating through the pseudoinverse⁴ A^\dagger . Fortunately, Lemma 1 shows that it is possible to replace A^\dagger by A^T without hurting the performance.

²Another approach is via linear programming.

³The subgradient at the origin can be any value in $[-1,1]$.

⁴One approach is to replace A^\dagger by an arbitrary matrix $B \in \mathbb{R}^{d \times m}$ to be learned from data. This approach performs worse than our design, as shown in Figure 3.

Lemma 1. For any vector $x \in \mathbb{R}^d$, and any matrix $A \in \mathbb{R}^{m \times d}$ ($m < d$) with rank m , there exists an $\tilde{A} \in \mathbb{R}^{m \times d}$ with all singular values being ones, such that the following two ℓ_1 -norm minimization problems have the same solution:

$$P_1 : \min_{x' \in \mathbb{R}^d} \|x'\|_1 \quad \text{s.t.} \quad Ax' = Ax. \quad P_2 : \min_{x' \in \mathbb{R}^d} \|x'\|_1 \quad \text{s.t.} \quad \tilde{A}x' = \tilde{A}x. \quad (11)$$

Furthermore, the projected subgradient update of P_2 is given as

$$x^{(t+1)} = x^{(t)} - \alpha_t(I - \tilde{A}^T \tilde{A})\text{sign}(x^{(t)}), \quad x^{(1)} = \tilde{A}^T \tilde{A}x. \quad (12)$$

A natural choice for \tilde{A} is $U(AA^T)^{-1/2}A$, where $U \in \mathbb{R}^{m \times m}$ can be any unitary matrix.

Lemma 1 essentially says that: 1) Instead of searching over *all* matrices (of size m -by- d), it is enough to search over a subset of matrices \tilde{A} , whose singular values are all ones. This is because A and \tilde{A} has the same recovery performance for ℓ_1 -minimization (this is true as long as \tilde{A} and A have the same null space). 2) The key benefit of searching over matrices with singular values being all ones is that the corresponding projected subgradient update has a simpler form: the annoying pseudoinverse term in (10) is replaced by a simple matrix transpose in (12).

3.2 Network Structure of ℓ_1 -AE

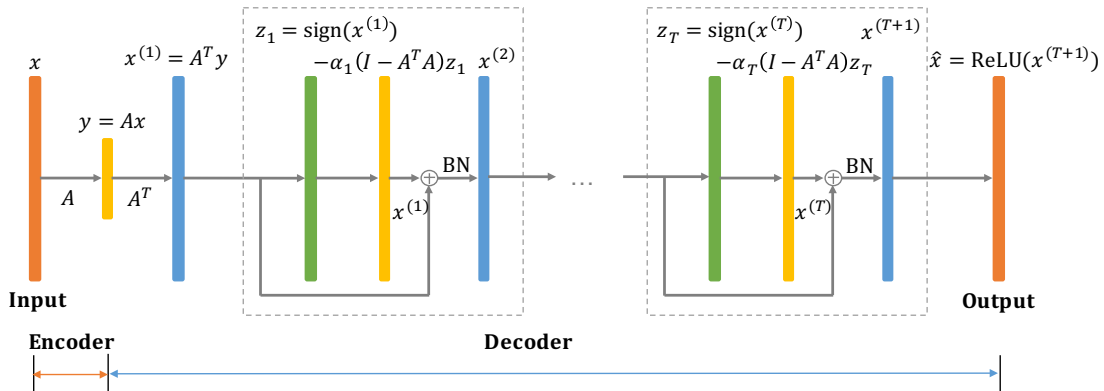


Figure 1: Network structure of the proposed autoencoder ℓ_1 -AE .

As shown in Figure 1, ℓ_1 -AE contains a simple linear encoder. When a data point $x \in \mathbb{R}^d$ comes, it is encoded as $y = Ax$, where $A \in \mathbb{R}^{m \times d}$ is the encoding matrix that will be learned from data. A decoder is then used to recover the original vector x from its embedding y .

The decoder network of ℓ_1 -AE consists of T blocks connected in a feedforward manner: the output vector of the t -th block is the input vector to the $(t + 1)$ -th block. The network structure inside each block is identical. Let $x^{(1)} = A^T y$. For $t \in \{1, 2, \dots, T\}$, if $x^{(t)} \in \mathbb{R}^d$ is the input to the t -th block, then its output vector $x^{(t+1)} \in \mathbb{R}^d$ is⁵

$$x^{(t+1)} = x^{(t)} - \alpha_t(I - A^T A)\text{sign}(x^{(t)}). \quad (13)$$

⁵By Lemma 1, ideally we should train our ℓ_1 -AE by enforcing the constraint that the matrices have singular values being ones. In practice, we do not enforce that during training. We empirically observe that the learned measurement matrix A is not far from the constraint set, as shown in Appendix D.6.

where $\alpha_1, \alpha_2, \dots, \alpha_T \in \mathbb{R}$ are scalar variables to be learned from data. We empirically observe that regularizing α_t to have the following form⁶ $\alpha_t = \beta/t$ for $t \in \{1, 2, \dots, T\}$ improves test accuracy. Here, $\beta \in \mathbb{R}$ is the only scalar variable to be learned from data. We also add a standard batch normalization (BN) layer [IS15] inside each block, because empirically it improves the test accuracy (see Figure 3). After T blocks, we use rectified linear units (ReLU) in the last layer⁷ to obtain the final output $\hat{x} \in \mathbb{R}^d$: $\hat{x} = \text{ReLU}(x^{(T+1)})$, where $x^{(T+1)} \in \mathbb{R}^d$ is the output vector of the T -th block.

It is worth noting that the low-rank structure of the weight matrix $I - A^T A$ in (13) is essential for reducing the computational complexity. A vanilla fully-connected layer would require a weight matrix of size $d \times d$, which is intractable if the input dimension d is high.

Given n unlabeled training examples $\{x_i\}_{i=1}^n$, we will train ℓ_1 -AE to minimize the average squared ℓ_2 reconstruction error between $x \in \mathbb{R}^d$ and $\hat{x} \in \mathbb{R}^d$:

$$\min_{A \in \mathbb{R}^{m \times d}, \beta \in \mathbb{R}} \frac{1}{n} \sum_{i=1}^n \|x_i - \hat{x}_i\|_2^2. \quad (14)$$

4 Experiments

We implement ℓ_1 -AE in Tensorflow 1.4. The code can be found at <https://github.com/wushanshan/L1AE>. The goal of this section is to demonstrate that ℓ_1 -AE is able to learn a good measurement matrix A for structured sparse datasets, when the standard ℓ_1 -minimization is used for decoding. Note that during the experiments, we use Gurobi (a commercial optimization solver) to solve the ℓ_1 -minimization problem.

4.1 Datasets and training

Dataset	Dimension	NNZs	Train / Valid / Test Size	Description
Synthetic1	1000	10	6000 / 2000 / 2000	1-block sparse with block size 10
Synthetic2	1000	10	6000 / 2000 / 2000	2-block sparse with block size 5
Amazon	15626	9	19661 / 6554 / 6554	1-hot encoded categorical data
RCV1	47236	76	13889 / 4630 / 4630	Text data with TF-IDF features

Table 1: Summary of the datasets. The column “NNZs” is the average number of nonzeros in every sample point. The validation set is used for parameter tuning and early stopping. We also experimented with power-law structured sparsity, see Appendix D.4.

Synthetic datasets. We generate two random datasets according to the block sparsity model [BCDH10]. Our first dataset (Synthetic1) is 1-block sparse with block size 10, while the second dataset (Synthetic2) is 2-block sparse with block size 5. Each sample is generated as follows: 1) choose a random support set from the block sparsity model⁸; 2) set the nonzeros to be uniformly distributed in $[0, 1]$.

⁶This form is sometimes called *square summable but not summable* [Boy14].

⁷This makes sense as we focus on nonnegative sparse vectors in this paper.

⁸A signal $x \in \mathbb{R}^d$ is called K -block sparse with block size J if it satisfies: 1) x can be reshaped into a matrix X of size $J \times N$, where $JN = d$; 2) every column of X acts as a group, i.e., the entire column is either zero or nonzero; 3) X has K nonzero columns, and hence x has sparsity KJ .

Real datasets. Our first dataset is from Kaggle “Amazon Employee Access Challenge”⁹. Each training example contains 9 categorical features. We use one-hot encoding to transform each example into a 15626-dimensional vector. Our second dataset is the Reuters Corpus Volume I (RCV1)¹⁰, a popular text dataset. Each training example has 47236 TF-IDF features. We use scikit-learn to fetch the training set of the RCV1 dataset, and then randomly split it into train/validation/test sets.

Training. We use SGD for training. Before training, we normalize every sample to have unit ℓ_2 norm. The parameters are initialized as follows: $A \in \mathbb{R}^{m \times d}$ is a random matrix generated by a truncated normal distribution with standard deviation $1/\sqrt{d}$; β is initialized as 1.0. The training parameters are given in Appendix B. Although standard convergence result for subgradient method [Boy14] indicates that the decoder’s depth T has a $O(1/\epsilon^2)$ dependence, in practice, a small value of T (e.g., $T = 10$) seems to be good enough.

4.2 Algorithms

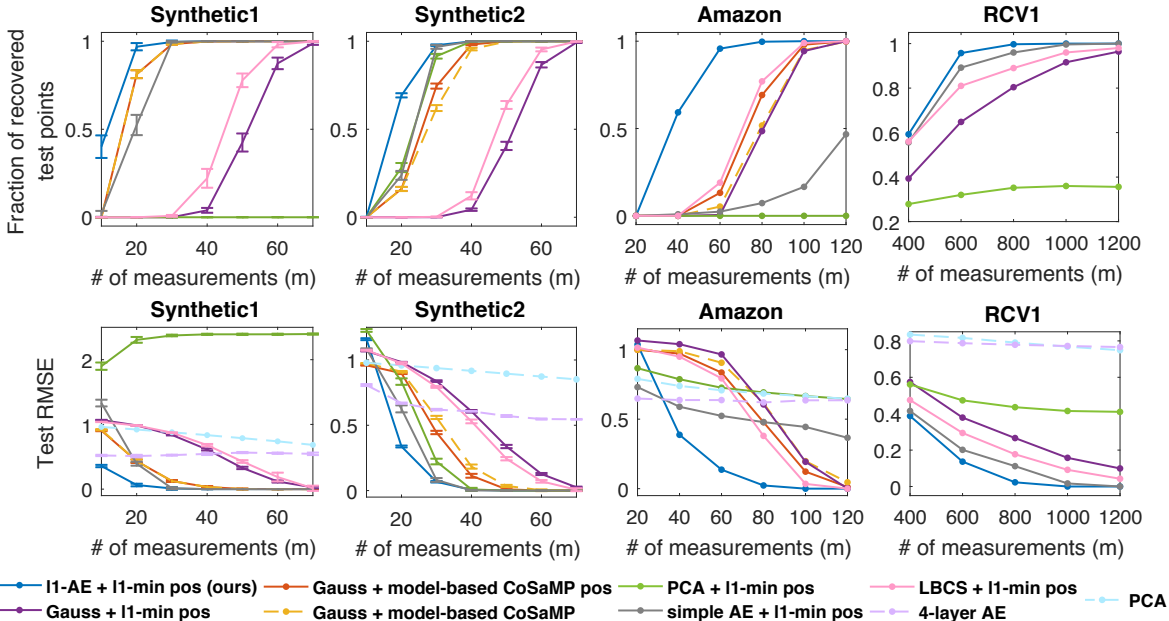


Figure 2: Recovery performance on the test set: fraction of exactly recovered data points (top row); reconstruction error (bottom row). Best viewed in color. We say that a vector x is exactly recovered by an algorithm if it produces a reconstruction \hat{x} that satisfies $\|x - \hat{x}\|_2 \leq 10^{-10}$. For Synthetic1 and Synthetic2, we plot the mean and standard deviation (indicated by the error bars) across 10 randomly generated datasets. Although the model-based CoSaMP decoder has more information about the given data (such as block sparsity and one-hot sparsity) than the ℓ_1 -minimization decoder, our “AE + ℓ_1 -min pos” still gives the best recovery performance across all datasets.

We compare 9 algorithms in terms of their recovery performance. The results are shown in

⁹<https://www.kaggle.com/c/amazon-employee-access-challenge>

¹⁰<http://scikit-learn.org/stable/datasets/rcv1.html>

Figure 2. All the algorithms follow a two-step *encoding* + *decoding* process.

- ℓ_1 -AE + ℓ_1 -min pos (our algorithm): After training an ℓ_1 -AE over the training set, we use the encoder matrix A as the measurement matrix. To decode, we use Gurobi (a commercial optimization solver) to solve the following optimization problem

$$\min_{x' \in \mathbb{R}^d} \|x'\|_1 \quad \text{s.t. } Ax' = y, x' \geq 0. \quad (15)$$

Since we focus on nonnegative sparse vectors in this paper, adding a positivity constraint improves the recovery performance¹¹ (see the comparisons given in Appendix D.3).

- Gauss + ℓ_1 -min pos / model-based CoSaMP / model-based CoSaMP pos: A random Gaussian matrix $G \in \mathbb{R}^{m \times d}$ with i.i.d. $\mathcal{N}(0, 1/m)$ entries is used as the measurement matrix¹². We experiment with three decoding methods: 1) Solve the optimization problem in (15); 2) Use the standard model-based CoSaMP algorithm (Algorithm 1 in [BCDH10]) as the recovery algorithm¹³; 3) We add a positivity constraint to the original model-based CoSaMP algorithm (see Appendix C), and use it as the decoding algorithm.
- PCA + ℓ_1 -min pos: We perform truncated singular value decomposition (SVD) on the training set, and use the top singular vectors as the measurement matrix. Decoding is performed via solving (15).
- PCA: We perform truncated SVD on the training set. Suppose $A \in \mathbb{R}^{m \times d}$ is top- m singular vectors, every vector $x \in \mathbb{R}^d$ in the test set is estimated by $A^T Ax$.
- Simple AE + ℓ_1 -min pos: We train a simple autoencoder: for an input vector $x \in \mathbb{R}^d$, the output is given as $\text{ReLU}(B^T Ax) \in \mathbb{R}^d$, where both $B \in \mathbb{R}^{m \times d}$ and $A \in \mathbb{R}^{m \times d}$ are learned from data. We use the same loss function as our autoencoder. After training, we use the learned A matrix as the measurement matrix. Decoding is performed by (15).
- LBCS + ℓ_1 -min pos: We implement the learning-based compressive subsampling (LBCS) method in [BLS⁺16]. The idea is to learn a subset (of size m) of coordinates (in the transformed space) that preserves the most energy. We focus on the average-case of LBCS, and use Gaussian matrix as the transformation matrix and basis pursuit as the decoder¹⁴.
- 4-layer AE: We train a standard 4-layer autoencoder, whose encoder network (and also decoder network) consists of two feedforward layers with ReLU activation. The dimension of the first (and the third) layer is tuned based on the performance on the validation set.

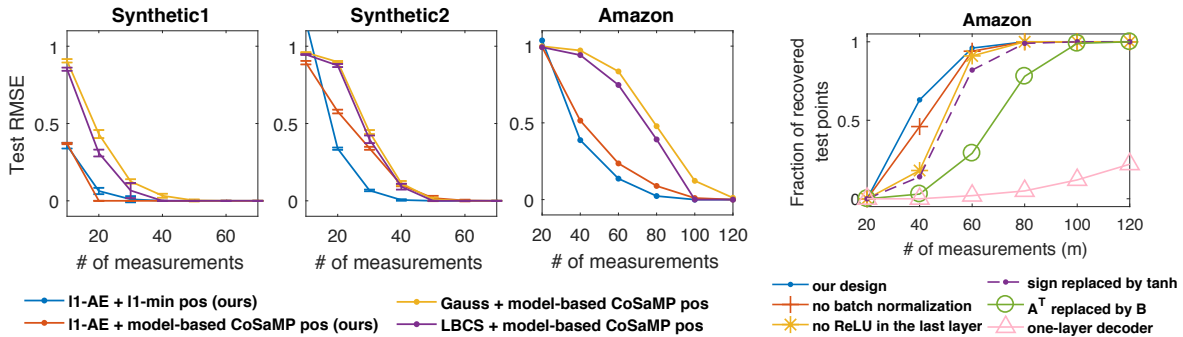


Figure 3: **Left three plots:** Recovery performance of “ ℓ_1 -AE + model-based CoSaMP pos” on the test set. Best viewed in color. Although ℓ_1 -AE is designed for the ℓ_1 -min decoder, the matrix learned from ℓ_1 -AE also improves the recovery performance when the decoder is model-based CoSaMP. **Right plot:** Recovery performance of “ ℓ_1 -AE + ℓ_1 -min pos” on the Amazon test set when we slightly change the decoder structure. Each change is applied in isolation.

4.3 Results

The experimental results are shown in Figure 2. Two performance metrics are compared. The first one is the fraction of exactly recovered test samples. We say that a vector x is exactly recovered by an algorithm if it produces an \hat{x} that satisfies¹⁵ $\|x - \hat{x}\|_2 \leq 10^{-10}$. The second metric is the root mean-squared error (RMSE) over the test set.

As shown in Figure 2, our algorithm “ ℓ_1 -AE + ℓ_1 -min pos” outperforms the other baselines over the four datasets. In other words, by adapting to the additional structure in the given data, we are able to compress the input vectors onto a smaller dimensional space. Our method also outperforms the other learning-based methods (i.e., PCA, LBCS, and Simple AE), which demonstrates the superior ability of ℓ_1 -AE in learning and exploiting structural information from data.

It is interesting to see that our algorithm outperforms model-based method [BCDH10], even though the model-based decoder has more information about the given data than the ℓ_1 -min decoder. We note that for the Amazon dataset, compared to “Gauss + model-based CoSaMP pos”, our method reduces the number of measurements needed for exact recovery by about 2x. This is possible because the model-based decoder only knows that the input vector

¹¹In fact, the sufficient and necessary condition (Theorem 3.1 of [KDXH11]) for exact recovery using (15) is weaker than the nullspace property (NSP) [Rau10] for a vanilla ℓ_1 -minimization.

¹²Additional experiments with random partial Fourier matrices [HR17] can be found in Appendix D.2.

¹³Since model-based CoSaMP requires to know the structured sparsity model, we cannot use it for the RCV1 dataset because it has no explicit sparsity model.

¹⁴We experimented with four variations of LBCS: two different basis matrices (random Gaussian matrix and DCT matrix), two different decoders (ℓ_1 -minimization and linear decoder). We found that the combination of Gaussian and ℓ_1 -minimization performs the best. See Appendix D.5 for a comparison of the four variations.

¹⁵As an iterative algorithm, the CoSaMP algorithm’s performance may depend on the halting criterion. In our experiments, we assume that it knows the original vector x (which is not possible in reality), and monitor the error $\|\hat{x} - x\|_2$ after each iteration. In other words, the performance of the CoSaMP algorithm shown in Figure 2 is its best performance regardless of the halting criterion.

comes from one-hot encoding, which is a *coarse* model for the underlying sparsity model. By contrast, our autoencoder learns the structure directly from the given data, and hence can capture *more accurate dependencies* between the features.

A natural question is whether the measurement matrix learned by ℓ_1 -AE can improve the recovery performance of the model-based decoding algorithm. As shown in Figure 3, the recovery performance of “ ℓ_1 -AE + model-based CoSaMP pos” is better than “Gauss + model-based CoSaMP pos”. This further demonstrates the benefit of learning an adaptive measurement matrix from data.

We now examine how slightly varying the decoder structure would affect the performance. We make the following changes to the decoder structure used for the Amazon dataset: 1) remove the BN layer; 2) remove the ReLU operation in the last layer; 3) change the nonlinearity from sign to tanh; 4) replace the A^T term in the decoder network by a matrix $B \in \mathbb{R}^{d \times m}$ that is learned from data; 5) use one-layer neural network as the decoder, i.e., set $T = 0$ in ℓ_1 -AE. Each change is applied in isolation. As shown in Figure 3, our design gives the best recovery performance among all the variations.

5 Conclusion

Combining ideas from compressed sensing, convex optimization and deep learning, we have proposed a novel unsupervised learning framework for high-dimensional sparse data. We have shown that ℓ_1 -AE is able to learn an efficient measurement matrix by adapting to the sparsity structure of the given data. This paper provides several interesting directions for future research. For example, the learned representation can be used in other machine learning tasks such as clustering, which prefers low-dimensional dense vectors over high-dimensional sparse vectors. Each column of the learned measurement matrix can be viewed as a feature embedding. We can incorporate ℓ_1 -AE into bigger supervised or unsupervised (e.g., generative model) systems.

References

- [ACCD13] Ery Arias-Castro, Emmanuel J Candès, and Mark A Davenport. On the fundamental limits of adaptive sensing. *IEEE Transactions on Information Theory*, 59(1):472–481, 2013.
- [AEB06] Michal Aharon, Michael Elad, and Alfred Bruckstein. k-svd: An algorithm for designing overcomplete dictionaries for sparse representation. *IEEE Transactions on Signal Processing*, 54(11):4311–4322, 2006.
- [AKNV18] Sanjeev Arora, Mikhail Khodak, Saunshi Nikunj, and Kiran Vodrahalli. A compressed sensing view of unsupervised text embeddings, bag-of-n-grams, and lstms. In *International Conference on Learning Representations (ICLR)*, 2018.
- [BCDH10] Richard G Baraniuk, Volkan Cevher, Marco F Duarte, and Chinmay Hegde. Model-based compressive sensing. *IEEE Transactions on Information Theory*, 56(4):1982–2001, 2010.
- [BD09] Thomas Blumensath and Mike E Davies. Iterative hard thresholding for compressed sensing. *Applied and Computational Harmonic Analysis*, 27(3):265–274, 2009.

- [BGKL15] Christos Boutsidis, Dan Garber, Zohar Karnin, and Edo Liberty. Online principal components analysis. In *Proceedings of the twenty-sixth annual ACM-SIAM symposium on Discrete algorithms (SODA)*, pages 887–901. Society for Industrial and Applied Mathematics, 2015.
- [BLS⁺16] Luca Baldassarre, Yen-Huan Li, Jonathan Scarlett, Baran Gözcü, Ilija Bogunovic, and Volkan Cevher. Learning-based compressive subsampling. *IEEE Journal of Selected Topics in Signal Processing*, 10(4):809–822, 2016.
- [Boy14] Stephen Boyd. Subgradient methods. *Notes for EE364b, Stanford University, Spring 2013–14*, 2014.
- [BSC13] Bubacarr Bah, Ali Sadeghian, and Volkan Cevher. Energy-aware adaptive bi-lipschitz embeddings. In *Proceedings of the 10th International Conference on Sampling Theory and Applications*, number EPFL-CONF-187483, 2013.
- [Can08] Emmanuel J Candès. The restricted isometry property and its implications for compressed sensing. *Comptes Rendus Mathématique*, 346(9-10):589–592, 2008.
- [CRT06] Emmanuel J Candès, Justin Romberg, and Terence Tao. Robust uncertainty principles: Exact signal reconstruction from highly incomplete frequency information. *IEEE Transactions on Information Theory*, 52(2):489–509, 2006.
- [DE03] David L Donoho and Michael Elad. Optimally sparse representation in general (nonorthogonal) dictionaries via ℓ_1 minimization. *Proceedings of the National Academy of Sciences*, 100(5):2197–2202, 2003.
- [DMM09] David L Donoho, Arian Maleki, and Andrea Montanari. Message-passing algorithms for compressed sensing. *Proceedings of the National Academy of Sciences*, 106(45):18914–18919, 2009.
- [Don06] David L Donoho. Compressed sensing. *IEEE Transactions on Information Theory*, 52(4):1289–1306, 2006.
- [DT05] David L Donoho and Jared Tanner. Sparse nonnegative solution of underdetermined linear equations by linear programming. *Proceedings of the National Academy of Sciences of the United States of America*, 102(27):9446–9451, 2005.
- [EBC⁺10] Dumitru Erhan, Yoshua Bengio, Aaron Courville, Pierre-Antoine Manzagol, Pascal Vincent, and Samy Bengio. Why does unsupervised pre-training help deep learning? *Journal of Machine Learning Research*, 11(Feb):625–660, 2010.
- [GL10] Karol Gregor and Yann LeCun. Learning fast approximations of sparse coding. In *Proceedings of the 27th International Conference on Machine Learning (ICML)*, pages 399–406, 2010.
- [GML⁺18] Baran Gözcü, Rabeeh Karimi Mahabadi, Yen-Huan Li, Efe Ilıcak, Tolga Çukur, Jonathan Scarlett, and Volkan Cevher. Learning-based compressive mri. *arXiv preprint arXiv:1805.01266*, 2018.

- [HIS14] Chinmay Hegde, Piotr Indyk, and Ludwig Schmidt. Approximation-tolerant model-based compressive sensing. In *Proceedings of the twenty-fifth annual ACM-SIAM symposium on Discrete algorithms (SODA)*, pages 1544–1561. SIAM, 2014.
- [Hot33] Harold Hotelling. Analysis of a complex of statistical variables into principal components. *Journal of educational psychology*, 24(6):417, 1933.
- [HR17] Ishay Haviv and Oded Regev. The restricted isometry property of subsampled fourier matrices. In *Geometric Aspects of Functional Analysis*, pages 163–179. Springer, 2017.
- [HRW14] John R Hershey, Jonathan Le Roux, and Felix Weninger. Deep unfolding: Model-based inspiration of novel deep architectures. *arXiv preprint arXiv:1409.2574*, 2014.
- [HS06] Geoffrey E Hinton and Ruslan R Salakhutdinov. Reducing the dimensionality of data with neural networks. *Science*, 313(5786):504–507, 2006.
- [HSYB15] Chinmay Hegde, Aswin C Sankaranarayanan, Wotao Yin, and Richard G Baraniuk. Numax: A convex approach for learning near-isometric linear embeddings. *IEEE Transactions on Signal Processing*, 63(22):6109–6121, 2015.
- [HXIW17] Hao He, Bo Xin, Satoshi Ikehata, and David Wipf. From bayesian sparsity to gated recurrent nets. In *Advances in Neural Information Processing Systems (NIPS)*, pages 5560–5570, 2017.
- [IS15] Sergey Ioffe and Christian Szegedy. Batch normalization: Accelerating deep network training by reducing internal covariate shift. In *Proceedings of the 32nd International Conference on Machine Learning (ICML)*, pages 448–456, 2015.
- [KDXH11] M Amin Khajehnejad, Alexandros G Dimakis, Weiyu Xu, and Babak Hassibi. Sparse recovery of nonnegative signals with minimal expansion. *IEEE Transactions on Signal Processing*, 59(1):196–208, 2011.
- [KW14] Diederik P Kingma and Max Welling. Auto-encoding variational bayes. In *The International Conference on Learning Representations (ICLR)*, 2014.
- [LC16] Yen-Huan Li and Volkan Cevher. Learning data triage: linear decoding works for compressive mri. In *ICASSP*, 2016.
- [LWZ17] Chris Junchi Li, Mengdi Wang, and Tong Zhang. Diffusion approximations for online principal component estimation and global convergence. In *Advances in Neural Information Processing Systems (NIPS)*, 2017.
- [MB17] Ali Mousavi and Richard G Baraniuk. Learning to invert: Signal recovery via deep convolutional networks. In *Proceedings of the International Conference on Acoustics, Speech, and Signal Processing (ICASSP)*, 2017.
- [MBPS09] Julien Mairal, Francis Bach, Jean Ponce, and Guillermo Sapiro. Online dictionary learning for sparse coding. In *Proceedings of the 26th Annual International Conference on Machine Learning (ICML)*, pages 689–696. ACM, 2009.

- [MDB17] Ali Mousavi, Gautam Dasarathy, and Richard G Baraniuk. Deepcodec: Adaptive sensing and recovery via deep convolutional neural networks. In *55th Annual Allerton Conference on Communication, Control and Computing*, 2017.
- [MMP⁺17] Morteza Mardani, Hatef Monajemi, Vardan Papyan, Shreyas Vasanaawala, David Donoho, and John Pauly. Recurrent generative adversarial networks for proximal learning and automated compressive image recovery. *arXiv preprint arXiv:1711.10046*, 2017.
- [MN14] Matthew L Malloy and Robert D Nowak. Near-optimal adaptive compressed sensing. *IEEE Transactions on Information Theory*, 60(7):4001–4012, 2014.
- [MPB15] Ali Mousavi, Ankit B Patel, and Richard G Baraniuk. A deep learning approach to structured signal recovery. In *Communication, Control, and Computing (Allerton), 2015 53rd Annual Allerton Conference on*, pages 1336–1343. IEEE, 2015.
- [MSC⁺13] Tomas Mikolov, Ilya Sutskever, Kai Chen, Greg S Corrado, and Jeff Dean. Distributed representations of words and phrases and their compositionality. In *Advances in neural information processing systems*, pages 3111–3119, 2013.
- [MSS⁺99] Sebastian Mika, Bernhard Schölkopf, Alex J Smola, Klaus-Robert Müller, Matthias Scholz, and Gunnar Rätsch. Kernel pca and de-noising in feature spaces. In *Advances in neural information processing systems*, pages 536–542, 1999.
- [NT09] Deanna Needell and Joel A Tropp. Cosamp: Iterative signal recovery from incomplete and inaccurate samples. *Applied and Computational Harmonic Analysis*, 26(3):301–321, 2009.
- [OF96] Bruno A Olshausen and David J Field. Emergence of simple-cell receptive field properties by learning a sparse code for natural images. *Nature*, 381(6583):607, 1996.
- [Pan16] Victor Y Pan. How bad are vandermonde matrices? *SIAM Journal on Matrix Analysis and Applications*, 37(2):676–694, 2016.
- [PSM14] Jeffrey Pennington, Richard Socher, and Christopher Manning. Glove: Global vectors for word representation. In *Proceedings of the 2014 conference on empirical methods in natural language processing (EMNLP)*, pages 1532–1543, 2014.
- [Rau10] Holger Rauhut. Compressive sensing and structured random matrices. *Theoretical Foundations and Numerical Methods for Sparse Recovery*, 9:1–92, 2010.
- [SBS15] Pablo Sprechmann, Alexander M Bronstein, and Guillermo Sapiro. Learning efficient sparse and low rank models. *IEEE Transactions on Pattern Analysis and Machine Intelligence*, 37(9):1821–1833, 2015.
- [SN11] Matthias W Seeger and Hannes Nickisch. Large scale bayesian inference and experimental design for sparse linear models. *SIAM Journal on Imaging Sciences*, 4(1):166–199, 2011.

- [TG07] Joel A Tropp and Anna C Gilbert. Signal recovery from partial information via orthogonal matching pursuit. *IEEE Transactions on Information Theory*, 53(12):4655–4666, 2007.
- [VLL⁺10] Pascal Vincent, Hugo Larochelle, Isabelle Lajoie, Yoshua Bengio, and Pierre-Antoine Manzagol. Stacked denoising autoencoders: Learning useful representations in a deep network with a local denoising criterion. *Journal of Machine Learning Research*, 11(Dec):3371–3408, 2010.
- [WBSD16] Shanshan Wu, Srinadh Bhojanapalli, Sujay Sanghavi, and Alexandros G Dimakis. Single pass pca of matrix products. In *Advances in Neural Information Processing Systems (NIPS)*, pages 2585–2593, 2016.
- [WLH16] Zhangyang Wang, Qing Ling, and Thomas Huang. Learning deep l0 encoders. In *Proceedings of the Thirtieth AAAI Conference on Artificial Intelligence*, 2016.
- [XWG⁺16] Bo Xin, Yizhou Wang, Wen Gao, David Wipf, and Baoyuan Wang. Maximal sparsity with deep networks? In *Advances in Neural Information Processing Systems (NIPS)*, pages 4340–4348, 2016.
- [ZG17] Jian Zhang and Bernard Ghanem. Ista-net: Iterative shrinkage-thresholding algorithm inspired deep network for image compressive sensing. *arXiv preprint arXiv:1706.07929*, 2017.

A Proof of Lemma 1

For convenience, we re-state Lemma 1 here and then give the proof.

Lemma. *For any vector $x \in \mathbb{R}^d$, and any matrix $A \in \mathbb{R}^{m \times d}$ ($m < d$) with rank m , there exists an $\tilde{A} \in \mathbb{R}^{m \times d}$ with all singular values being ones, such that the following two ℓ_1 -norm minimization problems have the same solution:*

$$P_1 : \min_{x' \in \mathbb{R}^d} \|x'\|_1 \quad \text{s.t. } Ax' = Ax. \quad P_2 : \min_{x' \in \mathbb{R}^d} \|x'\|_1 \quad \text{s.t. } \tilde{A}x' = \tilde{A}x. \quad (16)$$

Furthermore, the projected subgradient update of P_2 is given as

$$x^{(t+1)} = x^{(t)} - \alpha_t(I - \tilde{A}^T \tilde{A})\text{sign}(x^{(t)}), \quad x^{(1)} = \tilde{A}^T \tilde{A}x. \quad (17)$$

A natural choice for \tilde{A} is $U(AA^T)^{-1/2}A$, where $U \in \mathbb{R}^{m \times m}$ can be any unitary matrix.

Proof. To prove that P_1 and P_2 give the same solution, it suffices to show that their constraint sets are equal, i.e.,

$$\{x : Ax = Az\} = \{x : \tilde{A}x = \tilde{A}z\}. \quad (18)$$

Since $\{x : Ax = Az\} = \{z + v : v \in \text{null}(A)\}$ and $\{x : \tilde{A}x = \tilde{A}z\} = \{z + v : v \in \text{null}(\tilde{A})\}$, it then suffices to show that A and \tilde{A} have the same nullspace:

$$\text{null}(A) = \text{null}(\tilde{A}). \quad (19)$$

If v satisfies $Av = 0$, then $U(AA^T)^{-1/2}Av = 0$, which implies $\tilde{A}v = 0$. Conversely, we suppose that $\tilde{A}v = 0$. Since U is unitary, $AA^T \in \mathbb{R}^{m \times m}$ is full-rank, $(AA^T)^{(1/2)}U^T \tilde{A}v = 0$, which implies that $Av = 0$. Therefore, (19) holds.

The projected subgradient of P_2 has the following update

$$x^{(t+1)} = x^{(t)} - \alpha_t(I - \tilde{A}^T(\tilde{A}\tilde{A}^T)^{-1}\tilde{A})\text{sign}(x^{(t)}), \quad x^{(1)} = \tilde{A}^T(\tilde{A}\tilde{A}^T)^{-1}\tilde{A}z \quad (20)$$

Since $\tilde{A} = U(AA^T)^{-1/2}A$, we have

$$\tilde{A}\tilde{A}^T = U(AA^T)^{-1/2}AA^T(AA^T)^{-1/2}U^T = U(AA^T)^{-1/2}(AA^T)^{1/2}(AA^T)^{1/2}(AA^T)^{-1/2}U^T = I. \quad (21)$$

Substituting (21) into (20) gives the desired recursion:

$$x^{(t+1)} = x^{(t)} - \alpha_t(I - \tilde{A}^T \tilde{A})\text{sign}(x^{(t)}), \quad x^{(1)} = \tilde{A}^T \tilde{A}z. \quad (22)$$

□

B Training parameters

Table 2 lists the parameters used to train ℓ_1 -AE in our experiments. We explain the parameters as follows.

- Depth: The number of blocks in the decoder, indicated by T in Figure 1.

Dataset	Depth	Batch size	Learning rate	N_{\max}	$N_{\text{validation}}$	$N_{\text{no improve}}$
Toy	10	128	0.01	2e4	10	5
Synthetic1	10	128	0.01	2e4	10	5
Synthetic2	5	128	0.01	2e4	10	1
Amazon	60	256	0.01	2e4	1	1
RCV1	10	256	0.001	1e3	1	50

Table 2: Training parameters.

- Batch size: The number of training samples in a batch.
- Learning rate: The learning rate for SGD.
- N_{\max} : Maximum number of training epochs.
- $N_{\text{validation}}$: Validation error is computed every $N_{\text{validation}}$ epochs. This is used for early-stopping.
- $N_{\text{no improve}}$: Training is stopped if the validation error does not improve for $N_{\text{no improve}} * N_{\text{validation}}$ epochs.

C Model-based CoSaMP with additional positivity constraint

The CoSaMP algorithm [NT09] is a simple iterative and greedy algorithm used to recover a K -sparse vector from the linear measurements. The model-based CoSaMP algorithm (Algorithm 1 of [BCDH10]) is a modification of the CoSaMP algorithm. It uses the prior knowledge about the support of the K -sparse vector, which is assumed to follow a predefined *structured sparsity model*. In this section we slightly modify the model-based CoSaMP algorithm to ensure that the output vector follows the given sparsity model and is also *nonnegative*.

To present the pseudocode, we need a few definitions. We begin with a formal definition for the structured sparsity model \mathcal{M}_K and the sparse approximation algorithm \mathbb{M} . For a vector $x \in \mathbb{R}^d$, let $x|_{\Omega} \in \mathbb{R}^{|\Omega|}$ be entries of x in the index set $\Omega \in [d]$. Let $\Omega^C = [d] - \Omega$ be the complement of set Ω .

Definition 1 ([BCDH10]). *A structured sparsity model \mathcal{M}_K is defined as the union of m_K canonical K -dimensional subspaces*

$$\mathcal{M}_K = \bigcup_{m=1}^{m_K} \mathcal{X}_m \quad \text{s.t.} \quad \mathcal{X}_m = \{x : x|_{\Omega_m} \in \mathbb{R}^K, x|_{\Omega_m^C} = 0\}, \quad (23)$$

where $\{\Omega_1, \dots, \Omega_{m_K}\}$ is the set containing all allowed supports, with $|\Omega_m| = K$ for each $m = 1, \dots, m_K$, and each subspace \mathcal{X}_m contains all signals x with $\text{supp}(x) \subset \Omega_m$.

We define $\mathbb{M}(x, K)$ as the algorithm that obtains the best K -term structured sparse approximation of x in the union of subspaces \mathcal{M}_K :

$$\mathbb{M}(x, K) = \arg \min_{\bar{x} \in \mathcal{M}_K} \|x - \bar{x}\|_2. \quad (24)$$

Algorithm 1 Model-based CoSaMP with positivity constraint

Inputs: measurement matrix A , measurements y , structured sparse approximation algorithm \mathbb{M} Output: K -sparse approximation \hat{x} to the true signal x , which is assumed to be nonnegative $\hat{x}_0 = 0$, $r = y$; $i = 0$ {initialize}**while** halting criterion false **do**1. $i \leftarrow i + 1$ 2. $e \leftarrow A^T r$ {form signal residual estimate}3. $\Omega \leftarrow \text{supp}(\mathbb{M}_2(e, K))$ {prune residual estimate according to structure}4. $T \leftarrow \Omega \cup \text{supp}(\hat{x}_{i-1})$ {merge supports}5. $b|_T \leftarrow A_T^\dagger y$, $b|_{T^c} \leftarrow 0$ {form signal estimate by least-squares}6. $\hat{b} = \max\{0, b\}$ {set the negative entries to be zero}7. $\hat{x}_i \leftarrow \mathbb{M}(\hat{b}, K)$ {prune signal estimate according to structure}8. $r \leftarrow y - A\hat{x}_i$ {update measurement residual}**end while**return $\hat{x} \leftarrow \hat{x}_i$

We next define an enlarged set of subspaces \mathcal{M}_K^B and the associated sparse approximation algorithm.

Definition 2 ([BCDH10]). *The B -order sum for the set \mathcal{M}_K , with $B > 1$ an integer, is defined as*

$$\mathcal{M}_K^B = \left\{ \sum_{r=1}^B x^{(r)}, \quad \text{with } x^{(r)} \in \mathcal{M}_K \right\}. \quad (25)$$

We define $\mathbb{M}_B(x, K)$ as the algorithm that obtains the best approximation of x in the union of subspaces \mathcal{M}_K^B :

$$\mathbb{M}_B(x, K) = \arg \min_{\bar{x} \in \mathcal{M}_K^B} \|x - \bar{x}\|_2. \quad (26)$$

Algorithm 1 presents the model-based CoSaMP with positivity constraint. Comparing Algorithm 1 with the original model-based CoSaMP algorithm (Algorithm 1 of [BCDH10]), we note that the only different is that Algorithm 1 has an extra step (Step 6). In Step 6 we take a ReLU operation on b to ensure that \hat{x}_i is always nonnegative after Step 7.

We now show that Algorithm 1 has the same performance guarantee as the original model-based CoSaMP algorithm for structured sparse signals. Specially, we will show that Theorem 4 of [BCDH10] also applies to Algorithm 1. In [BCDH10], the proof of Theorem 4 is based on six lemmas (Appendix D), among which the only lemma that is related to Step 6-7 is Lemma 6. It then suffices to prove that this lemma is also true for Algorithm 1 under the constraint that the true vector x is nonnegative.

Lemma (Pruning). *The pruned approximation $\hat{x}_i = \mathbb{M}(\hat{b}, K)$ is such that*

$$\|x - \hat{x}_i\|_2 \leq 2\|x - b\|_2. \quad (27)$$

Proof. Since \hat{x}_i is the K -best approximation of \hat{b} in \mathcal{M}_K , and $x \in \mathcal{M}_K$, we have

$$\|x - \hat{x}_i\|_2 \leq \|x - \hat{b}\|_2 + \|\hat{b} - \hat{x}_i\|_2 \leq 2\|x - \hat{b}\|_2 \leq 2\|x - b\|_2, \quad (28)$$

where the last inequality follows from that $\hat{b} = \max\{0, b\}$, and $x \geq 0$. \square

The above lemma matches Lemma 6, which is used to prove Theorem 4 in [BCDH10]. Since the other lemmas (i.e., Lemma 1-5 in Appendix D of [BCDH10]) still hold for Algorithm 1, we conclude that the performance guarantee for structured sparse signals (i.e., Theorem 4 of [BCDH10]) is also true for Algorithm 1.

D Additional experimental results

D.1 A toy experiment

We use a simple example to illustrate that the measurement matrix learned from our autoencoder is adapted to the training samples. The toy dataset is generated as follows: each vector $x \in \mathbb{R}^{100}$ has 5 nonzeros randomly located in the first 20 dimensions; the nonzeros are random values between $[0,1]$. We train ℓ_1 -AE on a training set with 6000 samples. The parameters are $T = 10$, $m = 10$, and learning rate 0.01. A validation set with 2000 samples is used for early-stopping. After training, we plot the matrix A in Figure 4. The entries with large values are concentrated in the first 20 dimensions. This agrees with the specific structure in the toy dataset.

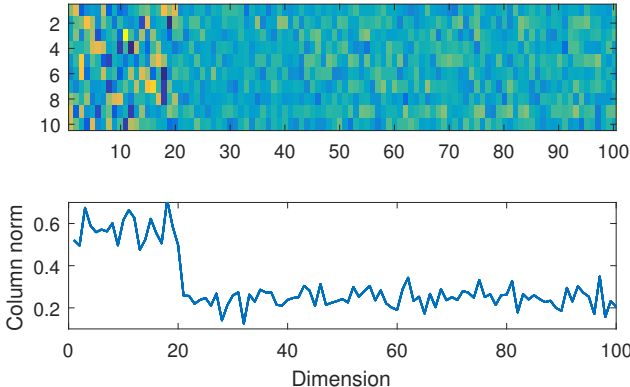


Figure 4: Visualization of the learned matrix $A \in \mathbb{R}^{10 \times 100}$ on the toy dataset: a color map of the matrix (upper), the column-wise ℓ_2 norm (lower). Every sample in the toy dataset has 5 nonzeros, located randomly in the first 20 dimensions.

D.2 Random partial Fourier matrices

Figure 5 is a counterpart of Figure 2. The only difference is that in Figure 5 we use random partial Fourier matrices in place of random Gaussian matrices. A random $M \times N$ partial Fourier matrix is obtained by choosing M rows uniformly and independently with replacement from the $N \times N$ discrete Fourier transform (DFT) matrix. We then scale each entry to have absolute

value $1/\sqrt{M}$ [HR17]. Because the DFT matrix is complex, to obtain m real measurements, we draw $m/2$ random rows from a DFT matrix to form the partial Fourier matrix.

A random partial Fourier matrix is a Vandermonde matrix. According to [DT05], one can exactly recover a k -sparse nonnegative vector from $2k$ measurements using a Vandermonde matrix [DT05]. However, the Vandermonde matrices are numerically unstable in practice [Pan16], which is consistent with our empirical observation. Comparing Figure 5 with Figure 2, we see that the recovery performance of a random partial Fourier matrix has larger variance than that of a random Gaussian matrix.

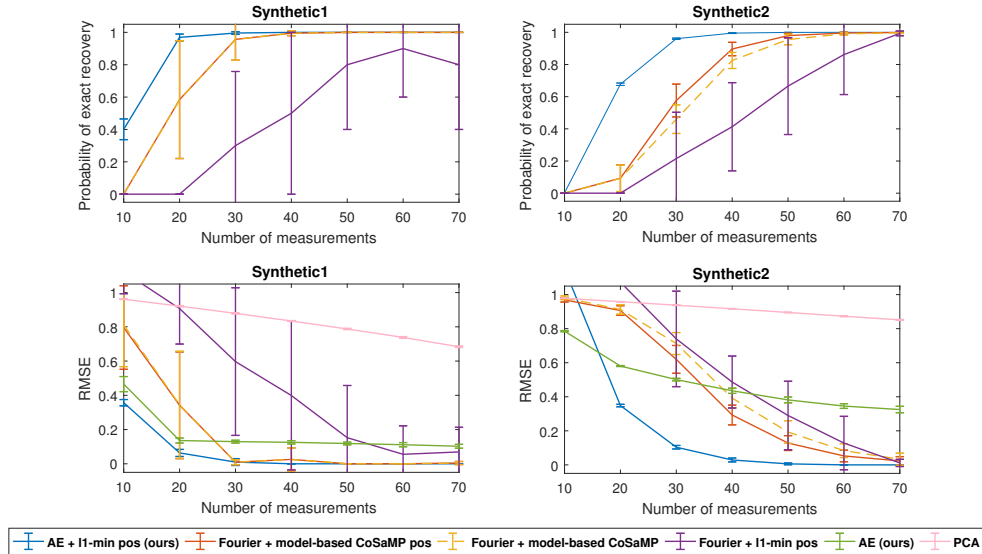


Figure 5: Recovery performance of random partial Fourier matrices. Best viewed in color. Similar to Figure 2, the error bars represent the standard deviation across 10 randomly generated datasets. We see that the recovery performance of a random partial Fourier matrix (shown in this figure) has a larger variance than that of a random Gaussian matrix (shown in Figure 2).

D.3 ℓ_1 -minimization with positivity constraint

We compare the recovery performance between solving an ℓ_1 -min (5) and an ℓ_1 -min with positivity constraint (15). The results are shown in Figure 6. We experiment with two measurement matrices: 1) the one obtained from training our autoencoder, and 2) random Gaussian matrices. As shown in Figure 6, adding a positivity constraint to the ℓ_1 -minimization improves the recovery performance for nonnegative input vectors.

D.4 Synthetic data with power-law sparsity

We generate a synthetic dataset following the power-law structured sparsity. Each vector is in \mathbb{R}^{1000} , with 10 nonzers on average. The i -th entry ($i = 1, 2, \dots, 1000$) is nonzero with probability proportional to $1/i$. The nonzero values are uniformly distributed in the interval

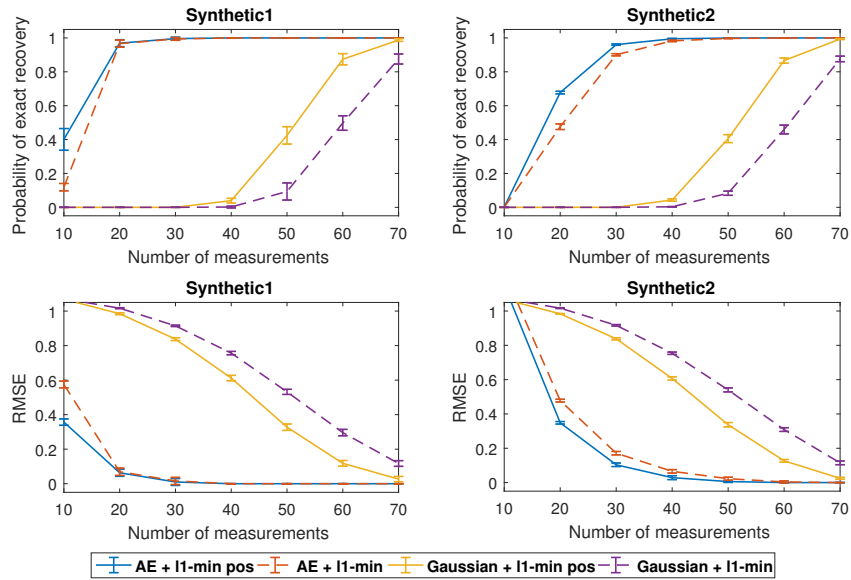


Figure 6: A comparison of the recovery performance between ℓ_1 -min (5) and the ℓ_1 -min with positivity constraint (15). The sparse recovery performance is measured on the test set. Best viewed in color. We plot the mean and standard deviation (indicated by the error bars) across 10 randomly generated datasets. Adding a positivity constraint to the ℓ_1 -minimization gives better recovery performance than a vanilla ℓ_1 -minimization.

$[0, 1]$. We generate 6000/2000/2000 samples as the training/validation/test set. The training parameters are the same as those used for Synthetic1 and Synthetic2 datasets (see Table 2). The experimental results are shown in Figure 7. Similar to Figure 2, using the measurement matrix learned from ℓ_1 -AE, we are able to compress the vectors onto a smaller dimension than using random matrices or matrices obtained from PCA. Note that model-based CoSaMP algorithm is not applicable in this case, where every support set is allowable but with different probability.

D.5 Additional experiments of LBCS

D.6 Singular values of the learned measurement matrices

We have shown that the measurement matrix obtained from training our autoencoder is able to capture the sparsity structure of the training data. We are now interested in looking at those data-dependent measurement matrices more closely. Table 3 shows that those matrices have singular values close to one. Recall that in Section 3.1 we show that matrices with all singular values being ones have a simple form for the projected subgradient update (12). Our decoder design is based on this simple update rule. Although we do not explicitly enforce this constraint during training, Table 3 indicates that the learned matrices are not far from the constraint set.

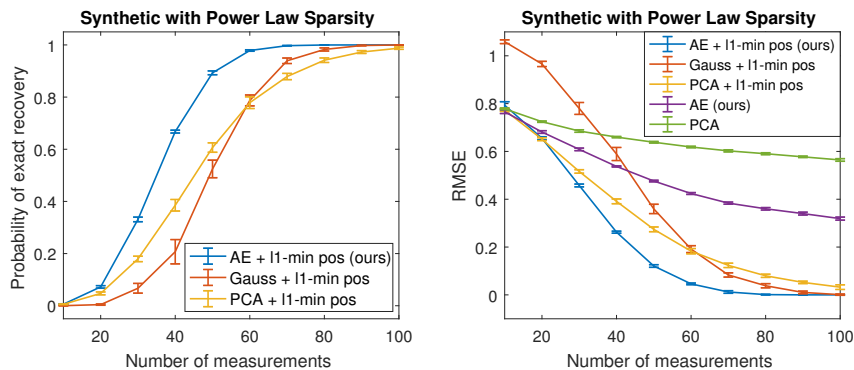


Figure 7: Recovery performance on the synthetic dataset with power-law structured sparsity. The performance is measured on the test set. Best viewed in color. We plot the mean and standard deviation (indicated by the error bars) across 10 randomly generated datasets. The proposed algorithm “AE + ℓ_1 -min pos” outperforms all the rest algorithms. Note that model-based CoSaMP algorithm is not applicable, because every support set is allowable.

Dataset	σ_{largest}	σ_{smallest}
Synthetic1	1.117 ± 0.003	0.789 ± 0.214
Synthetic2	1.113 ± 0.006	0.929 ± 0.259
Amazon	1.040 ± 0.021	0.804 ± 0.039
RCV1	1.063 ± 0.016	0.784 ± 0.034

Table 3: Range of the singular values of the measurement matrices $A \in \mathbb{R}^{m \times d}$ obtained from training ℓ_1 -AE . The mean and standard deviation is computed by varying the number of m (i.e., the “number of measurements” in Figure 2).

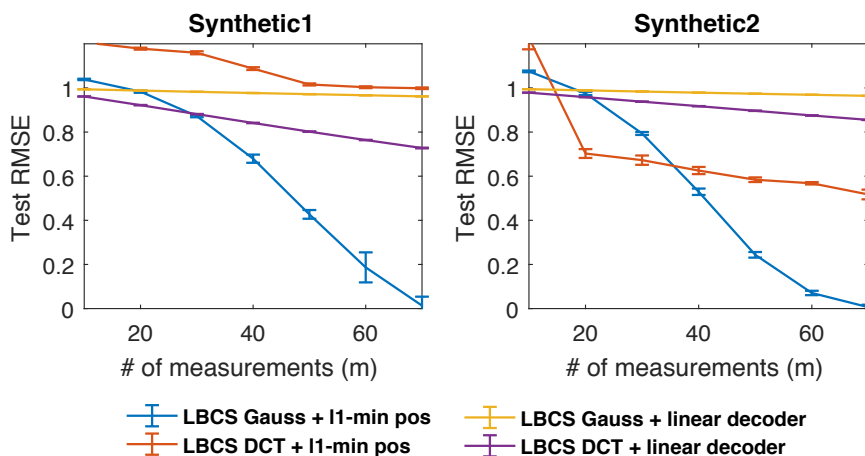


Figure 8: We compare four variations of the LBCS method proposed in [BLS⁺16, LC16]: two basis matrices (random Gaussian and DCT matrix); two decoders (ℓ_1 -minimization and linear decoding). The combination of “Gaussian + ℓ_1 -minimization” performs the best. Best viewed in color. For each method, we plot the mean and standard deviation (indicated by the error bars) across 10 randomly generated datasets.